[1] Vimal Gupta *
[2] Vimal Bibhu
[3] Sur Singh Rawat

Brain Tumor Detection and Segmentation using Improved Bat Algorithm with Improved Invasive Weed Optimization

Journal of Electrical Systems

Abstract: - Brain tumours are serious diseases that grow in the brain and are made up of a collection of abnormal and unwanted cells. Therefore, the use of magnetic resonance imaging (MRI) for segmentation and early detection of such tumors is more important to save lives. When it comes to finding people with brain tumors, MRI is very effective and has a slightly higher detection rate than other imaging tests. Detection of brain tumors is an important complex issue in medical imaging systems due to their size, appearance, and irregular shape. Detection of brain tumors is a difficult task with medical imaging systems. In order to address the above-said issue and to develop an effective brain tumor detection technique, an improved Bat algorithm with improved Invasive Weed Optimization algorithm has been proposed in this paper. The improved Invasive Weed Optimization (IIWO) approach has been utilized in the proposed IBIIW algorithm along with the improved Bat algorithm (IBA). In the proposed work weight factor which is used for classification has been improved. Extensive experiments has been performed and it suggests that, the use of MR imaging to segment tumors has a significant influence on early detection of brain cancers. In addition to this, with MR images, the deep learning-based technique produced better detection results. The proposed method has outperformed against the baseline methods in terms of accuracy, sensitivity, and specificity with remarkable results giving values of 0.9394, 0.9281, and 0.9165 respectively.

Keywords: Deep learning, Brain tumor detection, Data augmentation, Generative Adversarial Network (GAN), Bat Algorithm, MR Images (MRI).

I. INTRODUCTION

Computed tomography (CT) and magnetic resonance imaging (MRI) are additional methods for identifying brain cancers (CT). Magnetic resonance imaging (MRI) is one of the most widely used methods for detecting brain tumors (MRI), which produces detailed images of the brain. These methods are particularly successful in detecting brain tumors in patients and have a high detection rate. Modern imaging medicine now heavily relies on the magnetic resonance imaging (MRI) technique. Relevant clinical investigations have demonstrated that MRI is more accurate than CT for the diagnosis of intracranial brain tumors, with a 98 percent accuracy rate [18]. There are many advantages to using MRI imaging technology. Contrarily, people are more concerned about radiation even though this imaging method doesn't hurt the human body. It can be photographed, though, utilizing a range of factors, and this imaging strategy can provide a wealth of relevant information for diagnostic purposes in addition to being more beneficial and efficient for researching human metabolism and function. Additionally, MRI imaging technology offers a wealth of anatomical details on human soft tissues [1, 2, 3]. For full anatomical and functional evaluation, the latest magnetic resonance magnets feature a strong and uniform gradient. High image quality requires minimal patient movement, which can be achieved with either profound sedation or general anesthesia. Vectorcardiographic gating is used to freeze cardiac motion in all CMR experiments. In some patients, eliminating respiratory motion is also beneficial, therefore respiratory triggering or general anesthesia with breath retention for short periods of time are used [4]. The ability to separate brain tumors using MR images can help with diagnosis, growth rate prediction, and therapy planning. Meningiomas, for example, are straightforward to segment, but gliomas and glioblastomas are more difficult to find. These tumors (together with the edema that surrounds them) are frequently diffuse, poorly contrasted, and extend tentacle-like features that make segmentation difficult. Another major challenge in segmenting brain tumors is that they can occur practically anywhere in the brain and in almost any shape or size. White matter, grey matter, and cerebrospinal fluid are the three types of

[1] Department of Computer Science and Engineering, JSS Academy of Technical Education, Noida 201301, India.

[2] Department of Computer Science and Engineering, Noida international university, Greater Noida 201303, India. e-mail: vimalbibhu@gmail.com

[3] Department of Computer Science and Engineering, JSS Academy of Technical Education, Noida 201301, India. e-mail: sur.rawat@jssaten.ac.in

* Corresponding Author Email: vimalgupta@jssaten.ac.in

Copyright © JES 2024 on-line: journal.esrgroups.org

tissues that make up a healthy brain. The purpose of brain tumor segmentation is to find active tumorous tissue (vascularized or not), necrotic tissue, and edema, and to determine their position and extent (swelling near the tumor). Tumor segmentation is accomplished by recognizing aberrant areas in comparison to normal tissue. Because glioblastomas are infiltrative tumors, their borders are frequently blurry and difficult to discern from healthy tissue. Multiple MRI modalities are frequently used as a solution [5]. It is a difficult task to automate tumor identification and treatment planning. Existing semi-automated and fully automated tumor detection approaches are divided into two categories: generative and discriminative techniques. The discriminative approaches are based on diverse features such as texture, local histograms, and tensor eigen values [5], and do not rely on previous information. To address the limitations of standard segmentation approaches, this research proposes to design and create a residual neural network for tumor detection.

II. Related Work

Deep learning methods differ from conventional supervised machine learning methods in that they automatically learn an increasingly complex hierarchy of functions from the data rather than relying on manually created functions. Today, deep learning-based methods with BRATS datasets and their benchmarking systems are at the top of the competition. The fact that Deep CNNs are built by stacking multiple layers of convolution, including convolving signals or images in the kernel, and forming a robust and adaptive hierarchy of functions with discriminative models. There are still some difficulties, despite recent developments in these deep learning-based techniques. First, compared to other pattern recognition-based tasks, tumor segmentation [25] is a cognitively abnormal problem that is more challenging. Second, while most methods provided sufficient segmentation for HGG, LGG segmentation performance is generally poor. Third, the demarcation between the core tumor area and the enhanced infiltration area is still inadequate compared to complete tumor segmentation. Finally, existing CNN-based methods require significant computational resources, so more computationally efficient and memory-efficient development is still required. [6]. Deep learning models have recently gained popularity in the area of biomedical applications. There are numerous hidden layers that make up deep learning networks [7]. Additionally, this model automates the learning of the data records process.

2.1 Improved Bat Algorithm

In this algorithm, the weight Factor has been used

$$w_{itr} = \frac{(itr_{max} - itr)}{itr_{max}}(w_{max} - w_{min}) + w_{min} \quad (1)$$

where itr is the current iteration value, itr_{max} is the highest iteration number; w_{max} and w_{min} are the highest and lowest inertia weight factors respectively.

2.2 Improved Invasive Weed Optimization Algorithm

In this algorithm, the weight Factor has been used

$$WT_i = \frac{(T_i - T_d)*(T_i - T_{max})}{T_d * T_{max}} * W_{start} + \frac{(T_i)*(T_i - T_{max})}{T_d*(T_d - T_{max})} * WT_d + \frac{(T_i)*(T_i - T_d)}{T_{max}*(T_{max} - T_d)} * Wend \quad (2)$$

where, T_{max}: highest iteration number, T_d and WT_d are constants, W_{start}, and $Wend$ is initial inertia weight and end inertia weight respectively.

III. Proposed Deep Residual Architecture Based Brain Tumor Detection And Segmentation Using Improved Bat Algorithm With Improved Invasive Weed Optimization

This research's main aim is to design as well as develop a brain tumor diagnosis system with deep residual neural network. The series of steps followed for brain tumor segmentation are preprocessing, feature extraction, tumor segmentation, tumor detection, and data augmentation. The preprocessing module will first receive the input image and process it to remove any noise. After that, the tumor segmentation will be performed using the Spine-GAN algorithm [10]. Once the tumor segmentation is performed, the features, which include DFT features, Speeded-Up Robust Features (SURF) [11], and Local Optimal-Oriented Pattern (LOOP) features [12] and statistical characteristics, like mean, SD (Standard Deviation), Kurtosis, and entropy will be extracted for further processing. After feature extraction, data augmentation will be performed. Finally, the tumors will be detected using a Deep Residual Neural Network [13] where the training will be done based on an improved Bat Algorithm with Improved

Invasive Weed Optimization. The proposed IBIIW algorithm will be the integration of the Improved Bat algorithm (IBA) [19] and improved invasive weed (IIW) optimization [14, 15, 16, 17] [23, 24]. The proposed IBIIW algorithm will be applied in the PYTHON tool with the BRATS dataset. The performance of the suggested IBIIW optimization algorithms will be assessed with measures like accuracy, sensitivity, as well as specificity. Finally, the suggested methods and results will be compared to those of other current methodologies [20, 21, 22] in order to determine their effectiveness. The suggested Optimization-based Deep learning for Brain Tumor Detection is depicted in Fig 1. In the proposed work, the IDW (Inverse Distance Weighting) Interpolation Technique has been used.

$$x^* = \frac{wt_1 * x_1 + wt_2 * x_2 + wt_3 * x_3 + \ldots + wt_n * x_n}{wt_1 + wt_2 + wt_3 \ldots\ldots + wt_n} \quad (3)$$

$$wt = \frac{1}{d_{ix^*}^p} \quad (4)$$

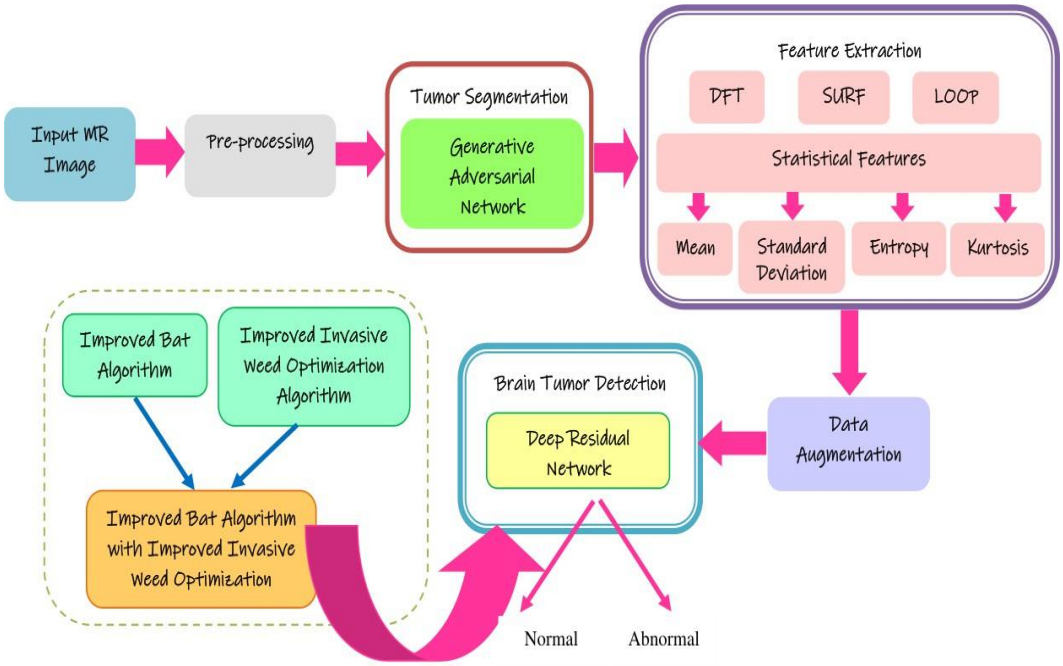

Fig. 1. Process flow diagram of the proposed Deep Residual network based on IBIIW for brain tumor detection

3.1 Pre-processing of the input image

The input picture is taken by the database and passed to the pre-processing step. The pre-processing step filters [26] the image more efficiently, improving the quality of the image and increasing the efficiency for further processing. There are trade-offs between resolution & SNR ("Signal-to-Noise Ratio") while taking MR pictures, which reduces image quality. The noise as well as the low contrast of MRI data makes it hard to exactly demarcate the region of interest between normal and tumor brain tissue. Therefore, image pre-processing is important to remove noise from the image as well as enhance the contrast between areas. This step removes existing noise in the image along with this it minimizes the effects of edge blur.

3.2 Tumor Segmentation using GAN

Fig 2 depicts the architecture of the GAN model. Here, generator G outputs a composite sample given the noise variable input z (z provides potential output diversity). It is trained to capture the actual data distribution so that the generated sample is as realistic as possible, that is, to trick the discriminator into providing a high probability. However, the following formula may be used to do this process:

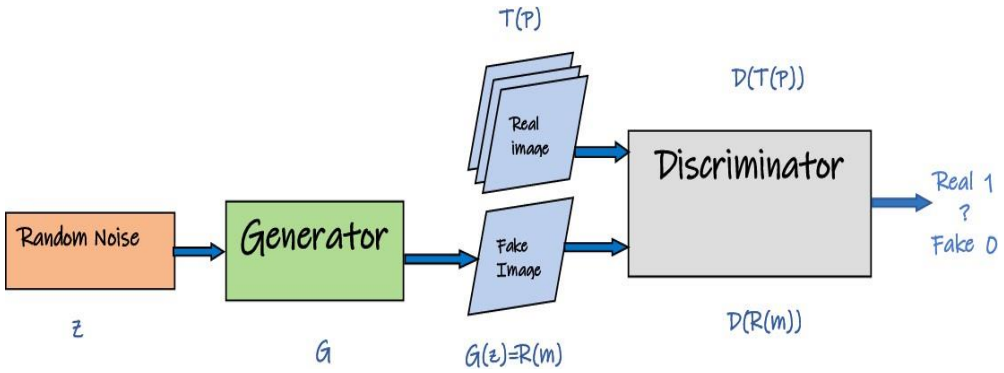

Fig. 2. Architecture of GAN

$$\min_R Y_R(T,R) = \min_R \left(G_{m\sim p_m}[log\left(1 - T\big(R(m)\big)\right)]\right) \quad (5)$$

Discriminator D "estimates the probability that a particular sample is from an actual data set. It acts as a critic and is optimized to discriminate between fake and real samples. For discriminators, the score for real samples (T(P)) is maximized, and the score for fake generated samples (R(m)) is minimized by minimizing (T(R(m))). However, the following equation allows this process.

$$\min_R Y_R(T,R) = \min_R \left(G_{m\sim p_m}[log\left(1 - T\big(R(m)\big)\right)]\right) \quad (6)$$

3.3 Feature extracted based on segmented result

Once the tumor segmentation will be performed, the features, which include DFT features, Speeded-Up Robust Features (SURF) [11] and Local Optimal-Oriented Pattern (LOOP) features [12] and statistical features, like mean, standard deviation, entropy, and Kurtosis will be extracted for further processing. The feature extraction mechanism [8] gained more importance in the area of medical imaging system due to high rate of accuracy measure and the effectiveness of the brain tumor detection. Some of features captured from segmented result include LOOP, SURF, DFT, and the statistical features.

LOOP: This feature represents the non-linear amalgamation of the LDP and the LBP features [9]. Let us consider intensity of the image as I at the pixel (u_i v_i) and the intensity of pixel in 3X3 neighborhood of (u_i v_i) is specified as I_j (j=0, 1, ... 7). The LOOP feature for the pixel (u_i v_i) is specified as

$$f_1 = \sum V\big(I_j - I_i\big)2^{w_j} \quad (7)$$

Where

$$V(K) = \begin{cases} 1 & K \geq 0 \\ 0 & otherwise \end{cases} \quad (8)$$

Here, f_1 denotes LOOP feature with the size of $[1\times 50]$.

SURF: Establishing a repeatable orientation using information from a circular zone surrounding the interest point is the first step. Then, a square region that is aligned to the desired orientation is used to extract the SURF descriptor.

$$f_2 = \sum_{i=0}^{x} \quad \sum_{i=0}^{y} I(x,y) \quad (9)$$

DFT: This feature is used to transform the segmented tumor result in to the vector of complex numbers using the below equation as,

$$f_3 = \sum_{r=0}^{U-1} s.e^{j.\frac{2\pi}{U}r} \quad (10)$$

Here, f_3 denotes DFT feature with the size of $[1\times 50]$.

Statistical features: The statistical features [8] captured from tumor result are explained as follows:

Mean: By adding the image's pixel counts to the total number of pixels, the mean feature of the image is calculated.

$$f_4 = \frac{1}{KXL}\sum_{y=0}^{K-1} \quad \sum_{z=0}^{L-1} s(y,z) \tag{11}$$

where, f_4 represents the mean feature with the dimension of $[1\times1]$.

Standard deviation: It is second central moment that shows the probability distribution such that it acts as the in homogeneity. Higher values indicate a higher intensity level and greater edge contrast [1] in the image.

$$f_5 = \sqrt{\frac{1}{KXL}\sum_{y=0}^{K-1} \quad \sum_{z=0}^{L-1}(s(y,z) - \mathrm{f}_4)^2} \tag{12}$$

where, f_5 indicates standard deviation feature with the dimension of $[1\times1]$.

Entropy:It is utilized to compute randomness of textural image and is given as,

$$f_6 = -\sum_{y=0}^{K-1} \quad \sum_{z=0}^{L-1} s(y,z) log_2 s(y,z) \tag{13}$$

where, f_6 indicates entropy feature with the dimension of $[1\times1]$.

Kurtosis:It is used to describe the shape of the segmented result's probability distribution and is specified as,

$$f_7 = \frac{1}{KXL}\frac{\sum(s(y,z)-\mathrm{f}_4)^4}{(\mathrm{f}_5)^4} \tag{14}$$

Here, f_6 denotes kurtosis feature with the dimension of $[1\times1]$. The feature vector employed to perform the brain tumor detection with the Deep Residual network is represented as,

$$f=\{f_1,\ldots f_7\} \tag{15}$$

Here, f indicates feature vector with the dimension of $[1\times154]$.

3.4 Data Augmentation

After extracting features from the segmented results, the data expansion process is performed more effectively and the results of tumor detection are improved. Data augmentation is the process of creating more samples by transforming training data to improve the robustness and accuracy of the classifier. Each feature extracted from the segmented result goes through a data expansion process to improve the dimension of the feature. Therefore, each feature is supplied individually to the data expansion module to produce the result of the feature in a larger dimension.

3.5 Architecture of Deep Residual Network

The deep learning model is effective at processing MR images in a way that produces accurate detection results with increased robustness and reliability. It accelerated training and cut down on training time. As a result, the deep learning model effectively addresses the computational complexity. A type of neural network called a deep residual network [6] is used to manage deep learning tasks and models in an efficient manner. This network has several layers, including a linear classifier, residual blocks, convolutional, and average pooling layer. Figure 3 displays the network architecture of the Deep Residual.

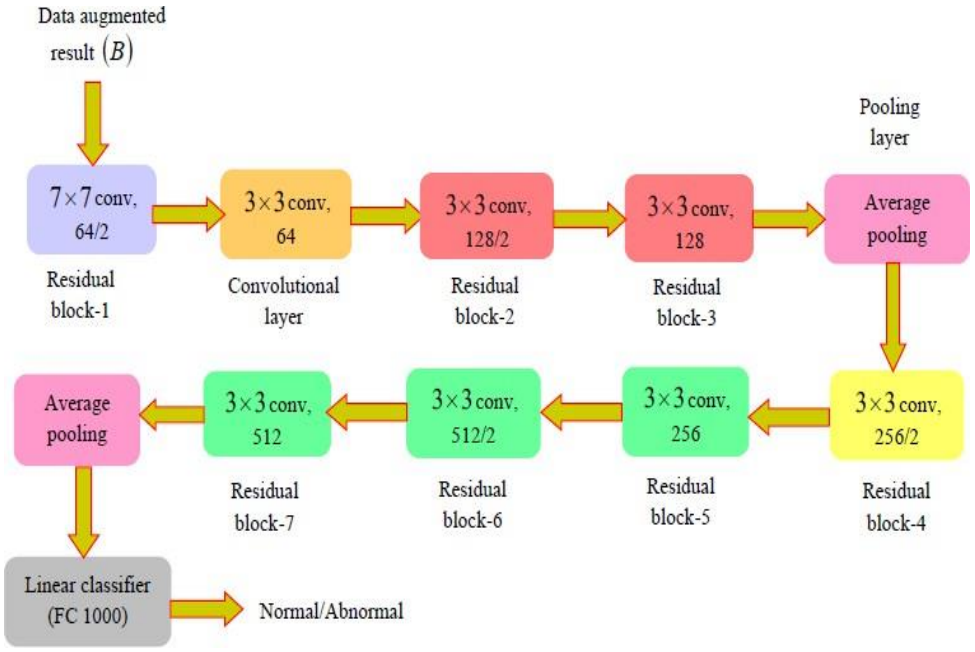

Fig. 3. Structure of Deep Residual Networks

3.6 Algorithmic Procedure of Ibiiw Algorithm

The algorithmic procesure of IBIIW Algorithm is shown in table 1. where 'ø' is the threshold value.T_max is the maximum no. of iterations. $globalbest_i$ is the global best position at the i number of iteration, $globalbest_{I-1}$ is the global best positions at the i-1 number of iteration

Algorithmic Procedure of IBIIW Algorithm

Step 1. Initialize the population,positions and velocities.

Step 2. Compute wT_i

Step 3. Bats Movement

Step 4. if $globalbest_i - globalbest_{i-1} > ø$ *W here,* o.1<ø> 1

global search based on Improved Invasive weed optimization algorithm

else

Local search based on Improved bat algorithm Step 5. Update the best bats

Step 5. Update the positions and velocities of bats Step 7. If $T_i > T_{max}$

Then go to step 2 else

end

IV. RESULTS AND DISCUSSION

This section covers the result of the developed detection scheme based on performance measures.

4.1 Experimental Design Setup

Using the Windows 10 operating system, 2GB of RAM, and an i-7 processor, the detection method is implemented in the Python tool. The experimental setup for the suggested techniques is shown in Table 1:

Table 1. Experimental Design Setup

Parameters	**Value**
Batch Size	128
No. of Filters	16
Learning Rate	1e-3
Activation Function	ReLU
Kernel Size	3
Maximum Iterations	100
Epochs	30

4.2 Dataset Description:

The created approach is implemented using the BRATS dataset, which can be found at https://www.med.upenn.edu/sbia/brats2018/data.html. The BRATS dataset is made up of multi-institutional pre-operative MRI images that are primarily utilized to segment heterogeneous brain malignancies like gliomas. In order to determine the clinical significance of the detection process, this dataset focuses on the prediction of a

4.3 Evaluation Metrics

The effectiveness of the developed scheme is assessed with metrics like sensitivity, accuracy, as well as specificity.
Accuracy: It illustrates the degree to which the computed value approaches the target value

$$ACC = \frac{TR_p + TR_n}{TR_p + TR_n + F_p + F_n} \quad (16)$$

WhereTRp denotes true positive, TRn signifies true negative, Fp specifies false positive, Fnillustrates false negative, and ACC represents accuracy.
Sensitivity: It is the ability of the test to accurately detect the presence of tumor and is given as,

$$SENS = \frac{TR_p}{TR_p + F_n} \quad (17)$$

Here, SENS denotes sensitivity.
Specificity: It is the probability of the test to exclude the tumor status and is specified as,

$$SENS = \frac{TR_p}{TR_p + F_n} \quad (18)$$

Where, SPECY signifies specificity.

4.4 Experimental Results

Fig. 4 depicts a sample picture of the detection model results from the BRATS dataset. Figures 4(a) depict the input picture as a result. Figures 4b show the pre-processed results of the input pictures. As a consequence, fig. 4c correspondingly, show the segmented findings.

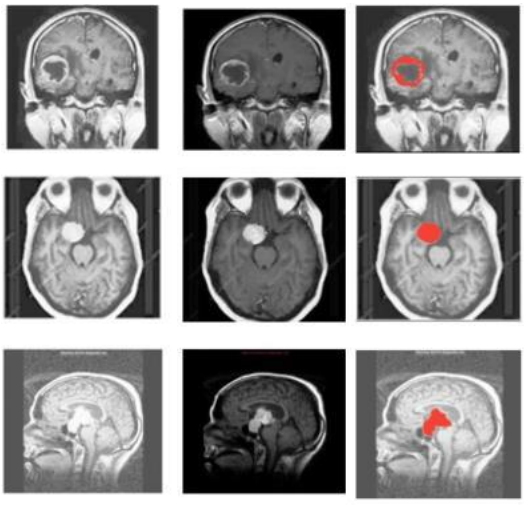

(a) ((b) (c)

Fig. 4. depicts a sample picture of the detection model results from the BRATS dataset. Figures 4(a) depict the input picture as a result. Figures 4b show the pre- processed results of the input pictures. As a consequence, fig. 4c correspondingly, show the segmented findings

V. RESULTS ANALYSIS

On the basis of the evaluation metrics, the performance analysis of the detection scheme is shown in the performance analysis section. The effectiveness of the detection scheme is assessed by comparing it to conventional methods such as Deep learning [16], Genetic algorithm edge detection (GA edge detection) [1], CNN (Convolutional Neural Network) [19], and SSAE (Stacked Sparse Autoencoder) [3] is shown in comparative analysis.

5.1 Performance Analysis

The suggested technique achieved the performance values on the basis of sensitivity accuracy, and specificity. Table 2. depicts a sensitivity, accuracy, and specificity analysis. The accuracy of the developed IBIIW-based Deep Residual network with the 10th, 20th, 30th, 40th, and 50th iterations is 0.7985, 0.8052, 0.8127, 0.8196, and 0.8447, respectively for 70% training values. The accuracy achieved using the suggested approach with the 10th, 20th, 30th, 40th, and 50th iterations is 0.8317, 0.8407, 0.8548, 0.8638, and 0.8908 correspondingly when training data is improved to an 80% value. However, considering the 10th iteration is 0.8784, the 20th iteration is 0.8835, the 30th iteration is 0.8998, the 40th iteration is 0.9042, and the 50th iteration is 0.9394 at 90% training samples.
Table 2. demonstrates the findings of the sensitivity measure analysis. The 10th iteration is 0.7589, the 20th iteration is 0.7651, the 30th iteration is 0.7749, the 40th iteration is 0.7829, and the 50th iteration is 0.8441, according to the developed method for 70% training samples. The sensitivity achieved by the proposed approach on the basis of the 10th, 20th, 30th, 40th, and 50th iterations is 0.820, 0.8289, 0.8375,0.8464, and 0.8721 respectively when using an 80% training value. When the training data value is 90%, the developed model's sensitivity with the 10th iteration is 0.8727, the 20th iteration is 0.8795, the 30th iteration is 0.8841, the 40th iteration is 0.8924, and the 50th iteration is 0.9165.

Table 2. Performance Analysis

Metrics	Training Dataset (%)	Iterations				
		10	20	30	40	50
Accuracy (ACC)	70	0.7985	0.8052	0.8127	0.8196	0.8447
	80	0.8317	0.8407	0.8548	0.8638	0.8908
	90	0.8784	0.8835	0.8998	0.9042	0.9394
Sensitivity (SENS)	70	0.7589	0.7651	0.7749	0.7829	0.8411
	80	0.8200	0.8289	0.8375	0.8464	0.8721
	90	0.8727	0.8795	0.8841	0.8924	0.9165
Specficity (SPECY)	70	0.7812	0.7934	0.8045	0.8125	0.8374
	80	0.8301	0.8378	0.8467	0.8545	0.8851
	90	0.8695	0.8765	0.8844	0.8924	0.9281

The analysis is illustrated with specificity in Table2. The developed method's specificity measure with the 10th, 20th, 30th, 40th, and 50th iterations is 0.7812, 0.7934, 0.8045, 0.8125, and 0.8374, correspondingly based on training data values of 70%.When the training data value is set to 80%, the proposed model's specificity computed with the 10th iteration is 0.8301, the 20th iteration is 0.8378, the 30th iteration is 0.8467, the 40th iteration is 0.8545, and the 50th iteration is 0.8851.As a result, when training data is improved to 90%,the proposed approach's specificity measure with 10th iteration is 0.8695, the 20th iteration is 0.8765, the 30th iteration is 0.8844, the 40th iteration is 0.8924, and the 50th iteration is0.9281.
When training data and iterations were increased, the suggested approach provided the highest levels of sensitivity, accuracy, and specificity. The suggested system has a "maximum sensitivity for 90% of the training data and iterations = 50. The efficient straining of the DRN classifier with the suggested IIB enhances the performance of the suggested system. The suggested systems offered maximum sensitivity, accuracy, as well

5.2 Comparative Analysis

Table 3. Demonstrate study with accuracy. Considering 70% as the training value, the accuracy calculated by GA edge detection, deep learning, CNN and SSAE is 0.6684, 0.7055, 0.7485 and 0.7615, while the developed Deep Residual network based on IBIIW presented 0.8447 accuracy. Nevertheless, the sensitivity calculated by GA edge detection, deep learning, CNN, SSAE, and the proposed approach is 0.6886, 0.7224, 0.7584, 0.7821 and 0.8411, correspondingly. Similarly, the specificity by GA edge detection, deep learning, CNN, SSAE, and the proposed

approach is 0.6917, 0.7082, 0.7551, 0.7767 and 0.8374 respectively. Fig 5 represents a comparison of the proposed model with Baseline Methods with 70% Training Samples.

Table 3. Comparative Analysis of Proposed Model against the Baseline Methods (70% Training Samples)

Dataset	Training (%)	Metrics	GA Edge Detect ion	Deep Learning	CNN	SSA E	Proposed IBIIW Based Deep Residual Network
Br ats	70	ACC	0.6684	0.7055	0.7485	0.7615	**0.8447**
		SENS	0.6886	0.7224	0.7584	0.7821	**0.8411**
		SPECY	0.6917	0.7082	0.7551	0.7767	**0.8374**

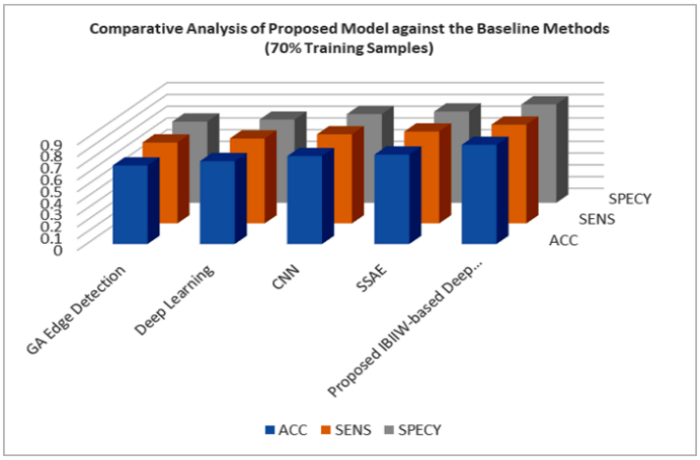

Fig. 5. Comparison of the proposed model with baseline methods with 70% training samples.

Table 4. Demonstrate analysis with accuracy. Considering 80% as the training value, the accuracy calculated by GA edge detection, deep learning, CNN and SSAE is 0.7288,0.7625,0.8048, and 0.8271, while the developed IBIIW-based deep residual network presented 0.8908 accuracies. Nevertheless, the sensitivity calculated by GA edge detection, deep learning, CNN, SSAE, and the proposed approach is 0.7086, 0.7321, 0.7786, 0.8122, and 0.8721 respectively. Similarly, the specificity by GA edge detection, deep learning, CNN, SSAE, and the proposed approach is 0.7061, 0.7585, 0.7751, 0.8123, and 0.8851 respectively. Fig 6 represents a comparison of the proposed model with baseline methods with 80% training samples.

Table 4. Comparative Analysis of Proposed Model against the Baseline Methods (80% Training Samples)

Data set	Training (%)	Metrics	GA Edge Detection	Deep Learning	CNN	SSAE	Proposed IBIIW Based Deep Residual Network
Br ats	80	ACC	0.7288	0.7625	0.8048	0.8271	**0.8908**
		SENS	0.7086	0.7321	0.7786	0.8122	**0.8721**
		SPECY	0.7061	0.7585	0.7751	0.8123	**0.8851**

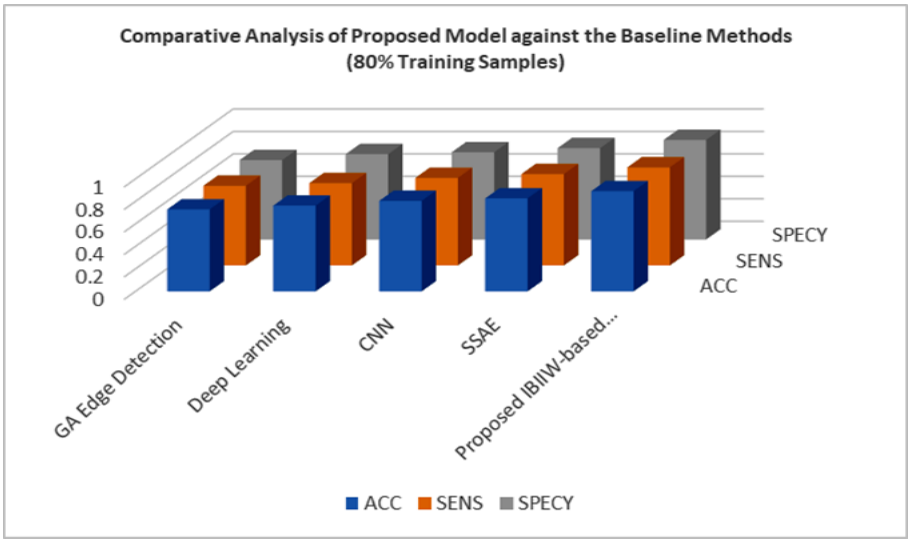

Fig. 6. Comparison of the proposed model with baseline methods with 80% training samples.

Table 5. Demonstrate analysis with accuracy. Considering 90% as the training value, the accuracy calculated by GA edge detection, deep learning, CNN and SSAE is 0.7500, 0.7746, 0.8259, and 0.8470, while the developed IBIIW-based Deep Residual network presented 0.9394 accuracy. Although, the sensitivity calculated by GA edge detection, deep learning, CNN, SSAE, and the proposed approach is 0.7224, 0.7520, 0.8050, 0.8184, and 0.9165 respectively. Similarly, the specificity by GA edge detection, deep learning, CNN, SSAE, and the proposed approach" is 0.7394, 0.7671, 0.7970, 0.8256, and 0.9281 respectively.

Table 5. Comparative Analysis of Proposed Model against the Baseline Methods (90% Training Samples)

Dataset	Training (%)	Metrics	GA Edge Detection	Deep Learning	CNN	SSAE	Proposed IBIIW Based Deep Residual Network
Brats	90	ACC	0.7500	0.7746	0.8259	0.8470	**0.9394**
		SEN S	0.7224	0.7520	0.8050	0.8184	**0.9165**
		SPE CY	0.7394	0.7671	0.7970	0.8256	**0.9281**

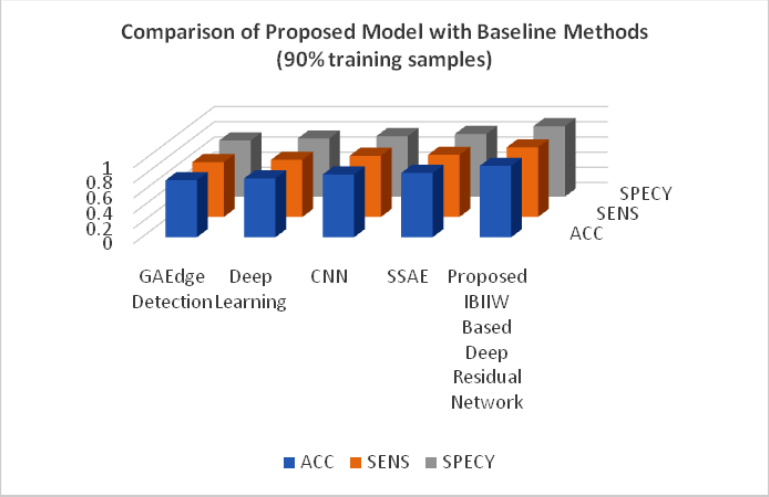

Fig. 7. Comparison of the proposed model with baseline methods with 90% training samples

VI. Conclusion and Future Scope

An effective method for detecting brain tumors is being developed using the Deep Residual Network Classifier in this study.DL classifiers are more efficient at performing segmentation as well as brain tumor detection tasks. The preprocessed phase efficiently corrects the picture and get rid of unwanted noise. This preprocessed image is then passed to the segmentation module, which uses the GAN approach to effectively divide the image and then capture

the exact area. The features associated with the segmented results are then extracted which also include LOOP,SURF,DFT,as well as statistical features.Finally,images of the brain are then classified as normal/abnormal using the Deep Residual Network.Extensive experiments have been per- formed and it advise that the suggested method has achieved remarkable performance in brain tumor detection mechanism in relation to the sensitivity, accuracy, and specificity with 0.8972, 0.8796, and 0.9042 values, correspondingly using the BRATS 2018. A future aspect of the study is to consider another DL classifier for segmenting and recognizing images of brain tumors to improve tumor classification performance.

REFERENCES

[1] Wang, W., Bu, F., Lin, Z. and Zhai, S., "Learning Methods of Convolutional Neural Network Combined With Image Feature Extraction in Brain Tumor Detection", IEEE Access, vol.8, pp.152659-152668, 2020.

[2] Tsolaki, E., Svolos, P., Kousi, E., Kapsalaki, E., Fezoulidis, I., Fountas, K., Theodorou, K., Kappas, C. and Tsougos, I., "Fast spec- troscopic multiple analysis (FASMA) for brain tumor classification: a clinical decision support system utilizing multi-parametric 3T MR data", International journal of computer assisted radiology and surgery, vol.10, no.7, pp.1149-1166, 2015.

[3] Bahadure, N.B., Ray, A.K. and Thethi, H.P., "Image analysis for MRI based brain tumor detection and feature extraction using biologically inspired BWT and SVM", International journal of biomedical imaging, 2017.

[4] Morris, S.A. and Slesnick, T.C., "Magnetic resonance imaging", Visual Guide to Neonatal Cardiology, pp.104-108, 2018.

[5] Havaei, M., Davy, A., Warde-Farley, D., Biard, A., Courville, A., Bengio, Y., Pal, C., Jodoin, P.M. and Larochelle, H., "Brain tumor segmentation with deep neural networks", Medical image analysis, vol.35, pp.18-31, 2017.

[6] Dong, H., Yang, G., Liu, F., Mo, Y. and Guo, Y., "Automatic brain tumor detection and segmentation using u-net based fully convolutional networks", In proceedings of annual conference on medical image understanding and analysis, pp. 506-517, 2017.

[7] Tog˘ac¸ar, M., Ergen, B. and Co¨mert, Z., "BrainMRNet: Brain tumor detection using magnetic resonance images with a novel convolutional neural network model", Medical hypotheses, vol.134, pp.109531, 2020.

[8] Saba, T., Mohamed, A.S., El-Affendi, M., Amin, J. and Sharif, M., "Brain tumor detection using fusion of hand crafted and deep learning features", Cognitive Systems Research, vol.59, pp.221-230, 2020.

[9] Chakraborti, T., McCane, B., Mills, S. and Pal, U., "Loop descriptor: Local optimal-oriented pattern", IEEE Signal Processing Letters, vol.25, no.5, pp.635-639, 2018.

[10] Tirupattur, P., Rawat, Y.S., Spampinato, C. and Shah, M., "Thoughtviz: Visualizing human thoughts using generative adversarial network", In Proceedings of the 26th ACM international conference on Multimedia, pp. 950-958, October 2018.

[11] HerbertBay, AndreasEss, TinneTuytelaars, LucVanGool "Speeded-Up Robust Features" Computer Vision and Image Understand- ing,Volume 110, Issue 3, June 2008, Pages 346-359

[12] Chakraborti, T., McCane, B., Mills, S. and Pal, U., "Loop descriptor: Local optimal-oriented pattern", IEEE Signal Processing Letters, vol.25, no.5, pp.635-639, 2018.

[13] Chen, Z., Chen, Y., Wu, L., Cheng, S. and Lin, P., "Deep residual network based fault detection and diagnosis of photovoltaic arrays using current-voltage curves and ambient conditions", Energy Conversion and Management, vol.198, pp.111793, 2019.

[14] Misaghi, M. and Yaghoobi, M., "Improved invasive weed optimization algorithm (IWO) based on chaos theory for optimal design of PID controller", Journal of Computational Design and Engineering, vol.6, no.3, pp.284-295, 2019.

[15] Avinash Gopal, quot;Hybrid classifier: Brain Tumor Classification and Segmentation using Genetic-based Grey Wolf optimization- quot;, Multimedia Research, vol.3, no.2, 2020.

[16] G.Gokulkumari, quot;Classification of Brain tumor using Manta Ray Foraging Optimization-based DeepCNNclassifierquot;, Mul- timedia Research, vol.3, no.4, 2020.

[17] Kumar, D.M., Satyanarayana, D. and Prasad, M.G., "MRI brain tumor detection using optimal possibilistic fuzzy C-means clustering algorithm and adaptive k-nearest neighbor classifier", Journal of Ambient Intelligence and Humanized Computing, vol.12, no.2, pp.2867-2880, 2021.

[18] Dolz, J., Laprie, A., Ken, S., Leroy, H.A., Reyns, N., Massoptier, L. and Vermandel, M., "Supervised machine learning-based classification scheme to segment the brainstem on MRI in multicenter brain tumor treatment context", International journal of computer assisted radiology and surgery, vol.11, no.1, pp.43-51, 2016.

[19] Yang, X.S., "A new metaheuristic bat-inspired algorithm", In Nature inspired cooperative strategies for optimization (NICSO 2010), pp. 65 -74, 2010.

[20] Saba, T., Mohamed, A.S., El-Affendi, M., Amin, J. and Sharif, M., "Brain tumor detection using fusion of hand crafted and deep learning features", Cognitive Systems Research, vol.59, pp.221-230, 2020.

[21] Amin, J., Sharif, M., Raza, M., Saba, T., Sial, R. and Shad, S.A., "Brain tumor detection: A long short- term memory (LSTM)-based learning model", Neural Computing and Applications, vol.32, no.20, pp.15965- 15973, 2020.

[22] Amin, J., Sharif, M., Gul, N., Raza, M., Anjum, M.A., Nisar, M.W. and Bukhari, S.A.C., "Brain tumor detection by using stacked autoencoders in deep learning", Journal of medical systems, vol.44, no.2, pp.1-12, 2020.

[23] S. Rawat, S. K. Verma and Y. Kumar, "Infrared small target detection based on Non-convexTriple Tensor Factorization," IET image processing, vol. 15, no. 2, pp. 556-570, 07-02-2021.

[24] S. Rawat, S. K. Verma and Y. Kumar, "Reweighted infrared patch image model for small target detection based on non-convex p-norm minimisation and TV regularisation," IET image processing, vol. 14, no. 9, pp. 1937–1947, 2020